Vertical profiles of lung deposited surface area concentration of particulate matter measured with a drone in a street canyon

Heino Kuuluvainen[a,*], Mikko Poikkimäki[a], Anssi Järvinen[a], Joel Kuula[b], Matti Irjala[c], Miikka Dal Maso[a], Jorma Keskinen[a], Hilkka Timonen[b], Jarkko V. Niemi[d], and Topi Rönkkö[a]

[a] *Aerosol Physics, Faculty of Natural Sciences, Tampere University of Technology, Tampere, Finland*
[b] *Atmospheric Composition Research, Finnish Meteorological Institute, Helsinki, Finland*
[c] *Aeromon Ltd., Helsinki, Finland*
[d] *Helsinki Region Environmental Services Authority (HSY), Helsinki, Finland*

Abstract

The vertical profiles of lung deposited surface area (LDSA) concentration were measured in an urban street canyon in Helsinki, Finland, by using an unmanned aerial system (UAS) as a moving measurement platform. The street canyon can be classified as an avenue canyon with an aspect ratio of 0.45 and the UAS was a multirotor drone especially modified for emission measurements. In the experiments of this study, the drone was equipped with a small diffusion charge sensor capable of measuring the alveolar LDSA concentration of particles. The drone measurements were conducted during two days on the same spatial location at the kerbside of the street canyon by flying vertically from the ground level up to an altitude of 50 m clearly above the rooftop level (19 m) of the nearest buildings. The drone data were supported by simultaneous measurements and by a two-week period of measurements at nearby locations with various instruments. The results showed that the averaged LDSA concentrations decreased approximately from 60 $\mu m^2/cm^3$ measured close to the ground level to 36–40 $\mu m^2/cm^3$ measured close to the rooftop level of the street canyon, and further to 16–26 $\mu m^2/cm^3$ measured at 50 m. The high-resolution measurement data enabled an accurate analysis of the functional form of vertical profiles both in the street canyon and above the rooftop level. In both of these regions, exponential fits were used and the parameters obtained from the fits were thoroughly compared to the values found in literature. The results of this study indicated that the role of turbulent mixing caused by traffic was emphasized compared to the street canyon vortex as a driving force of the dispersion. In addition, the vertical profiles above the rooftop level showed a similar exponential decay compared to the profiles measured inside the street canyon.

Keywords: urban air quality, street canyon, aerosol, lung deposited surface area, vertical profile

Capsule: The high-resolution vertical profiles of lung deposited surface area obtained in this study are valuable with respect to exposure estimations, urban planning, and urban air quality models.

*Corresponding author
Email address: heino.kuuluvainen@tut.fi (Heino Kuuluvainen)

1. Introduction

Street canyons are important microenvironments in urban areas with respect to the dispersion of traffic emissions and human exposure. Pedestrians, cyclists, and people inside vehicles may be exposed to relatively high concentrations of particles and gaseous pollutants on the ground level of street canyons because of the reduced natural ventilation (Kumar et al., 2011; Vardoulakis et al., 2003). Vertical dispersion of pollutants affects the human exposure in buildings above the ground level and contributes to regional background concentrations as well as to the global atmospheric effects of anthropogenic emissions. According to Monks et al. (2009), the characterization of the vertical profiles in urban areas and street canyons is crucial in determining pollution transport from the urban area to the regional scale. Understanding of the vertical dispersion in street canyons also provides a possibility of improvements in urban planning, building ventilation, and indoor air quality (Ai and Mak, 2015).

The fine particulate matter, i.e. the particles with a diameter smaller than 2.5 µm (PM2.5), has been estimated to cause about 3.3 million premature deaths per year worldwide (Lelieveld et al., 2015). The problem is emphasized nowadays in Asia but also, in spite of the strict emission and air quality standards, still recognized in Western countries (Beelen et al., 2014). The mass of fine particles has been widely monitored in urban areas all over the world (Cheng et al., 2016) and shown to correlate with the incidence of cardiopulmonary diseases (Silva et al., 2013). In addition to the negative health effects, aerosols emitted from anthropogenic sources have also an impact on global climate (Rotstayn et al., 2009). In order to better understand the urban air quality with respect to the particulate matter and the effects of anthropogenic sources on global climate, a lot of different measurements conducted in urban environments have been reported, including particle number concentrations and number size distributions (Shi et al., 1999; Pant and Harrison, 2013; Pirjola et al., 2012), as well as chemical composition of particles (Putaud et al., 2004; Pirjola et al., 2017).

Recently, an increasing number of studies have reported surface area related quantities measured in urban areas. The reason for this trend can be found in toxicological studies where the surface area of particles has been shown to correlate with negative health effects better than the mass and number concentrations (Brown et al., 2001; Oberdörster et al., 2005). One of the most common surface related metric is the lung deposited surface area (LDSA) concentration that can be defined separately for the alveolar or trancheobronchial regions of lungs. The alveolar LDSA concentration has been found to be on average between 10 and 89 $\mu m^2/cm^3$ at urban background measurement stations located in different Western cities (Reche et al., 2015). According to a recent study by Kuuluvainen et al. (2016), traffic related particle modes dominate the size distribution of the LDSA and the average concentrations are usually at the highest at busy traffic sites.

The interest towards street canyons as significant microenvironments in urban areas has resulted in various measurements and development of models. It is commonly known that the highest concentrations of fine particles in urban areas usually exist in closed street canyons with relatively high and long buildings parallel to the street (Kumar et al., 2011; Pirjola et al., 2012). The basic dispersion of aerosol particles and other pollutants in a street canyon is

characterized by the vortex caused by the predominant wind above the building rooftop level and the turbulent mixing affected by bypassing vehicles (Qin and Kot, 1993). Kumar et al. (2009b) compared the performance of three different street canyon models including an operational street pollution model (OSPM) (Berkowicz, 2000), a semi-empirical box model, and a computational fluid dynamics (CFD) model. They found that the OSPM and box-based models were able to predict the similar shape of concentration profiles corresponding to pseudo-simultaneously measured values reported by Kumar et al. (2008b). Both of these models include calibration parameters based on experimental data from various field studies. The vertical profile of pollutant concentrations in a street canyon have also shown to follow an exponential form by multiple other studies. In a theoretical study (Huang, 1979), two wind tunnel experiments (Hoydysh and Dabberdt, 1988; Dabberdt and Hoydysh, 1991), and four field measurements studies (Capannelli et al., 1977; Zoumakis, 1995; Chan and Kwok, 2000; Vardoulakis et al., 2002), the concentrations were found to be the highest near the canyon bottom with a decreasing gradient towards the rooftop level.

A lack of experimental data or uncertainties related to the available data often restrict the evaluation of street canyon models. Several studies have reported particle concentrations and other pollutants measured at the ground and rooftop level of street canyons (Väkevä et al., 1999; Kukkonen et al., 2001; Pakkanen et al., 2003; Kumar et al., 2009a). The decrease of concentrations with the increasing altitude has been evident. Marini et al. (2015) conducted a measurement campaign with simultaneous aerosol particle measurements at three or four different heights on both sides of a symmetric street canyon and pointed out the strong influence of wind conditions on the particle concentrations in the canyon. It is noteworthy that unlike inert gases, such as carbon dioxide (CO_2), aerosols consist of particles of different sizes and composition, which may behave differently and interact with each other during dispersion and dilution processes (Kumar et al., 2008b; Imhof et al., 2005). Some measurements of carbon dioxide have been conducted at different heights up to 30 m in a lattice tower located in a street canyon with a rooftop level at the height of 15 m (Vogt et al., 2006). However, these results cannot directly be applied for particulate matter because of the inert nature of carbon dioxide and its relatively high and variable background levels compared to the ambient values in urban environments.

In general, the vertical concentration profiles of particulate matter and other pollutants can be measured with stationary or moving measurement platforms installed onto the walls of buildings and other constructions, or with flying measurement platforms. The above-mentioned studies reporting particle and CO_2 concentrations in street canyons are examples of stationary measurements. On the other hand, Imhof et al. (2005) measured particle concentrations and size distributions by using an elevator installed into a tower as a moving measurement platform at an open motorway environment. Recently, the development of unmanned aerial systems (UAS) or unmanned aerial vehicles (UAV), commonly known as drones, has enabled the measurement of vertical profiles especially by using sensor-type instruments with a light weight and a high time resolution. Villa et al. (2016) reviewed the use of drones in the air quality research and they found that the field is in its early stages of development. Most of the studies reporting measurements with a drone are focused

on meteorological parameters, such as temperature and relative humidity, and they have been performed by using fixed-wing drones that are not applicable for measuring vertical profiles close to the ground level (Elston et al., 2015). Only a few studies have reported measurements of particulate matter with a drone. Brady et al. (2016) demonstrated the performance of a rotary-wing drone equipped with an optical particle counter and a CO_2 sensor for vertical gradient measurements at the surf zone of an ocean. In a recent study by Villa et al. (2017), the vertical profiles of particle number concentration were measured with a drone adjacent to a motorway by using a sensor, based on the diffusion charging of particles.

The aim of this study was to investigate the vertical profiles of lung deposited surface area concentration in an urban street canyon. Measurements were performed with a miniature electrical particle sensor installed into a multirotor drone that was operated from the ground level to an altitude clearly above the rooftop level of the street canyon. The obtained vertical profiles were supported by stationary measurements at different heights and ground level measurements at nearby locations. The experimental data were analyzed further by using exponential fits and parametrization, the aim of which was to compare the results to previous studies. Altogether, this study demonstrates the performance of a drone in an urban street canyon environment for measurements of fine particles.

2. Methods

Measurements were carried out in a busy street canyon in Helsinki next to an urban supersite air quality measurement station (Mäkelankatu 50; 60°11′N, 24°57′E) operated by the Helsinki Region Environmental Services Authority (HSY). The location of the measurement station is shown on the map in Fig. 1a and 1b. The supersite measurement station consists of a container (length 8.0 m, width 1.7 m, height 2.7 m) that is equipped with the standard air quality measurement devices and other instrumentation. All the inlets for the measuring devices are located on the top of the container approximately at a height of 2.8 m from the ground level. The drone measurements were carried out right next to the measurement station during two days, on November 14th and 15th, 2016. These measurement days are referred as Day 1 and Day 2, respectively. In addition to them, stationary measurements at two different heights were carried out during the afternoon on November 17th, referred as a stationary day, and a two-week period of measurements between 7th and 23rd. In addition to the measurements in the street canyon, simultaneous measurements were carried out at an urban background measurement station in Kumpula (SMEAR III station; 60°12′N, 24°57′E; 30 m above sea level) (Järvi et al., 2009), seen on the map in Fig. 1a.

Figure 1c shows a schematic cross-section of the street canyon. The street Mäkeänkatu is one of the main streets in Helsinki aligned in a northwest–southeast direction at the measurement station. The average traffic volume is 28 100 vehicles per weekday (11 % heavy duty vehicles). As seen in Fig. 1b and 1c, the measurement station is located on the southwest side of the street at the kerbside between the sidewalk and roadway. The street consists of a sidewalk and three lanes for both directions for which the outermost lane is reserved for buses and taxis. In the middle, there is a green zone with two tram lines surrounded by trees. The

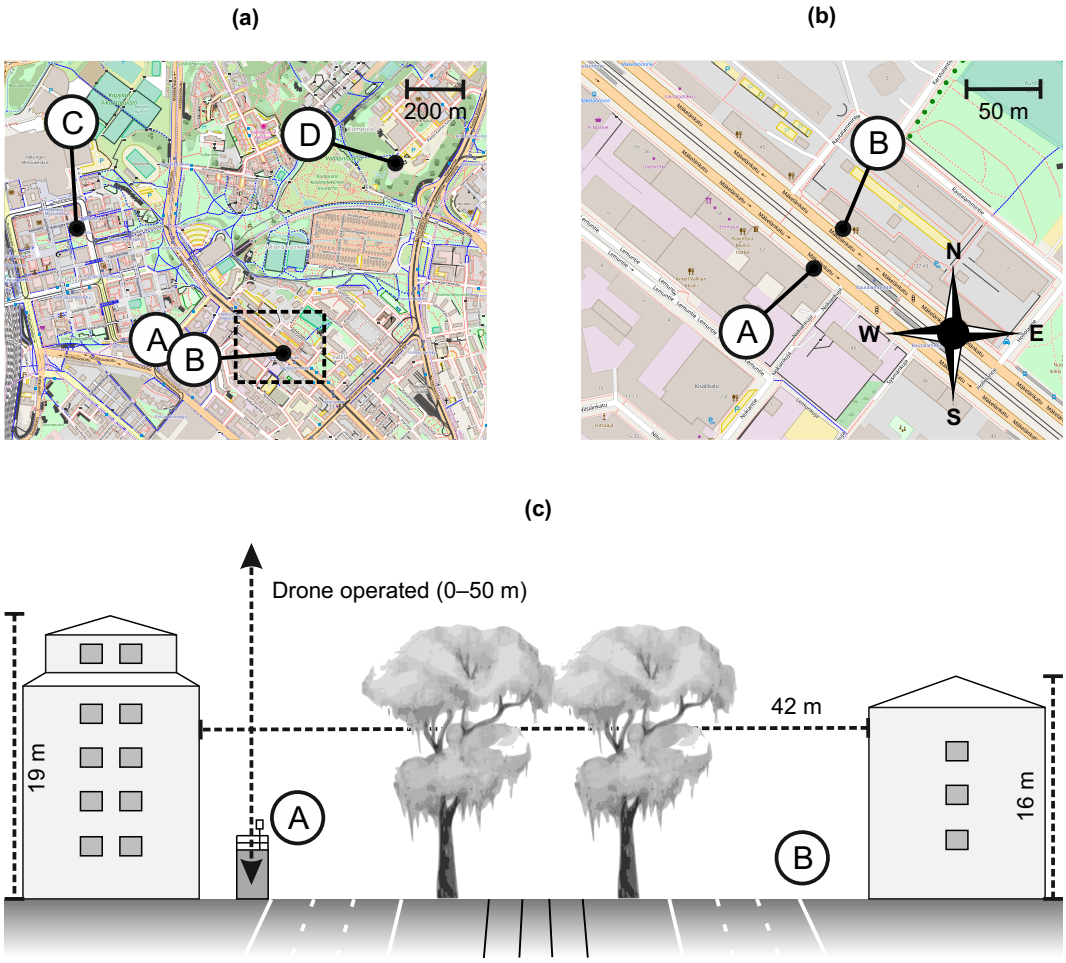

Figure 1: (a–b) The measurement locations in the street canyon (A and B), the location of the weather station (C), and the location of the urban background measurement station (D) on the map. (c) The exact locations (A and B) with respect to the cross-section of the street canyon. Also the building heights and the operation zone of the drone are shown. The measurement station is seen on the left. (a–b) ©OpenStreetMap contributors.

width of the street canyon is 42 m, and the heights of the buildings next to the measurement station and on the other side of the street are 19 and 16 m, respectively. We used the height of the buildings next to the measurement station and the place for the drone measurement as the canyon height. The ratio of the canyon height H and width W is commonly known as an aspect ratio (AR = H/W) that was 0.45 for this canyon. Usually, if the aspect ratio for a street canyon is below 0.5, the canyon can be classified as an avenue canyon. The drone was operated vertically starting from the ground on the southeast side of the measurement station up to an altitude of 50 m. During the drone measurements, simultaneous reference measurements were carried out with different instruments at the measurement station, on the other side of the street at the kerbside, and at the urban background measurement station. In addition, meteorological data, including the wind speed and direction, was measured at

a weather station located on a rooftop of a building at the height of 50 m from the ground level about one kilometer from the measurement station (Fig. 1a). These wind conditions can be assumed to represent the average wind conditions above the rooftop level at the street canyon.

The unmanned aerial system (UAS) used in the experiments was a multicopter manufactured by VideoDrone Finland Ltd. (Fig. S2). The model was X8, which means that the UAS had 8 motors in 4 pairs at the end of the grid bars. The UAS had been modified for emission measurements by Aeromon Ltd. by replacing the main payload of the UAS with a sensor unit, which in these measurements contained an onboard computer, network modems, GPS (global positioning system) antenna, and sensors for humidity, temperature, and pressure. The data of this unit consists of sensor reading paired with time and location from GPS and all the data were also sent forward to cloud service for visualization in real time. The pressure sensor was used as an altimeter its accuracy was ± 0.12 hPa corresponding approximately to an accuracy of ± 1 m in altitude. In order for the results to represent an altitude dependency, the air sample was taken outside of the UAS air flow caused by rotors. The sample to the particle sensor was taken through a Tygon E-3603 (Saint-Gobain Performance Plastics) tubing of 70 cm that was upheld by a hollow carbon fiber stick (Fig. S2). In the measurements, the drone was flown with an approximate velocity of 1 m/s from the ground level to an altitude of 50 m, which is clearly above the roof level of the nearby buildings. The lowest point between subsequent up-and-down flights was approximately at a height of 2 m. The drone was able to operate 3–5 subsequent up-and-down flights before the battery had to be changed or recharged. Altogether, 48 up-and-down flights were conducted during the two days.

The particle sensor installed into the drone was a Partector (Naneos GmbH) originally introduced by Fierz et al. (2014). The Partector is based on the diffusion charging of particles and the measurement of induced current with an electrometer. The output current signal of the instrument is calibrated to measure the alveolar lung deposited surface area (LDSA) concentration. The weight of the Partector is only 400 g, the time resolution 1 s, and it can be operated as much as 15 hours without recharging the battery, which makes it suitable for drone measurements. The sample flow of the Partector is 0.5 lpm, and the diffusion losses in the sample line of the drone measurement were estimated to be negligible. Also another similar sensor was used in the measurements. The sensor used in the drone is referred as Partector 1 and the other sensor is referred as Partector 2. Both the sensors were used simultaneously in the stationary measurements in a mast located at the top of the measurement station during few hours in the afternoon. Partector 1 was installed at a height of 2.8 m and Partector 2 at a height of 5.6 m. Because Partector 2 was recently calibrated by the manufacturer, it was used as a reference instrument for other instruments.

In addition to these two devices, several other instruments were used in the measurements. An electrical low pressure impactor (ELPI+, Dekati Ltd.) measured continuously during the campaign at the measurement station. The ELPI+ measures the aerodynamic size distribution of particles with a high time resolution and a detailed description of the instrument is given by Järvinen et al. (2014). Kuuluvainen et al. (2016) used the older version

of the instrument for measuring the LDSA concentrations and size distributions in an urban environment based on a field calibration. Another hand-held sensor similar to the Partector called a DiSCmini (Testo Ltd.) (Fierz et al., 2011) was used to measure the LDSA on the other side of the street (B) during the drone measurements. The DiSCmini was placed in a vehicle parked at the kerbside and the inlet of the sampling line was at a height of one meter from the ground level. Furthermore, a Pegasor AQ Urban sensor (Pegasor Ltd.) measured continuously at the top of the measurement station during the campaign and another similar sensor measured at the urban background measurement station in Kumpula (see location D in Fig. 1a). A predecessor of this sensor has been used previously to measure the LDSA in an urban environment by Järvinen et al. (2015). The time resolution of all these instruments was 1 s and a synoptic view of the instruments is shown in the supplementary material (Table S1). The devices Partector 1, Partector 2, ELPI+, and DiSCmini were installed to the same sampling line close to the Pegasor sensor located on the top of the container during the period from 18th to 23rd November. Thus, this period was used for the inter-comparison and field calibration of the instruments.

The obtained measurement data on the vertical concentration profiles were fitted with a mathematical equation to find a functional form for the LDSA concentration versus the measurement altitude. A simple exponential function has been suggested for the concentration of gaseous pollutants (Murena and Vorraro, 2003) as well as particle number concentration in a street canyon (Kumar et al., 2008a) and traffic intersections (Goel and Kumar, 2016). In this study, we formulate it as

$$C_z = C_{\mathrm{E,grd}} \exp(-k \cdot z^*) + C_{\mathrm{BG,str}}, \tag{1}$$

where C_z is the concentration at an altitude z and $C_{\mathrm{E,grd}} (= C_{\mathrm{grd}} - C_{\mathrm{BG,str}})$ is considered to be the concentration at the ground level resulting from ground level emissions. In other words, it is the ground level concentration C_{grd} substracted by the background concentration $C_{\mathrm{BG,str}}$ in the street canyon. The variable $z^* (= z/H)$ is the dimensionless altitude, which is the altitude z normalized by the street canyon heigth H. The exponential decay of the concentration can be characterized by the dimensionless decay coefficient $k (= k_1 \cdot H)$, where k_1 is the exponential decay coefficient in m^{-1}. The decay coefficient combines both meteorological and topographical parameters. A similar exponential expression as in Eq. (1) can be used to fit the measurement data above the rooftop level

$$C_z = C_{\mathrm{E,rft}} \exp(-k \cdot (z^* - 1)) + C_{\mathrm{BG,urb}}. \tag{2}$$

As a modification to Eq. (1), the z^* -axis is shifted in Eq. (2) by the dimensionless canyon height ($= 1$) to set the exponent term $\exp(-k \cdot (z^* - 1))$ to unity at the rooftop level instead of the ground level. This shift affects only the meaning of the parameter $C_{\mathrm{E,rft}} (= C_{\mathrm{rft}} - C_{\mathrm{BG,urb}})$, which is now the concentration at the rooftop level resulting from the street canyon emissions. However, the shift has no effects on the decay coefficient k or background concentration C_{BG}. The vertical profiles for Day 1 and Day 2 were divided into two regions: the region inside the street canyon below the rooftop level and the region over the rooftop level. The parameter values were acquired for $C_{\mathrm{E,grd}}$, k, $C_{\mathrm{BG,str}}$ inside the street canyon and for $C_{\mathrm{E,rft}}$, k, $C_{\mathrm{BG,urb}}$

above the rooftop level, along with the confidence bounds for these three parameter fits by using a MATLAB function `cftool`.

3. Results and discussion

Figure S1 found in the supplementary material shows a comparison of the instrument responses based on the field measurement data. All the data were validated and averaged over 10 min. Since Partector 2 was chosen to be the reference instrument, calibration factors were calculated for other instruments. The calibration factor (CF) for an instrument was defined as the LDSA concentration measured by Partector 2 divided by the simultaneous output signal of the instrument in question. As seen in Fig. S1, there were only small changes as a function of the LDSA concentration measured by the reference instrument seen in the calibration factors of different instruments. This indicates that the instrument responses were very similar with each other for these traffic related particles measured in the street canyon environment in these conditions. As a result of the comparison, the average calibration factors were used to calibrate and correct the output signals (LDSA in $\mu m^2/cm^3$ or electric current in pA) of all the instruments to be comparable with the LDSA measured by Partector 2. These factors were 1.18, 1.00, 30.3 $\mu m^2/(cm^3 pA)$, and 132 $\mu m^2/(cm^3 pA)$ for Partector 1, DiSCmini, ELPI+, and Pegasor AQ Urban, respectively.

The statistics of the measured LDSA values is important with respect to the averaging and comparison of different time series. Figure 2 illustrates the statistics of the LDSA values with a histogram, in which the number of observations per hour is presented as a function of the LDSA concentration. The distributions are shown with geometric mean, median, (arithmetic) mean, and geometric standard deviation values for the two-week period of measurements and, as an example, for the stationary measurements at the height of 2.8 m. As seen in this figure with a logarithmic x-axis, both the distributions seem to be close to a log-normal distribution. In the distribution for the two-week period, a slightly asymmetric shape can be seen, due to the strong diurnal variations and polarization of concentrations to high-traffic and low-traffic periods. The distribution for the stationary measurement includes data of only a few hours measured during an afternoon and the concentrations seem to be more precisely log-normally distributed. However, the geometric means and geometric standard deviations represent well the statistical characteristics of both of these example distributions. Therefore, the geometric mean and geometric standard deviation were used in the further analysis and averaging of the data.

The drone measurements were carried out during two days and the stationary measurements at different heights during one day. In order to estimate the representativeness of these measurement days with respect to the two-week period, Fig. 3 shows the diurnal variation of the LDSA concentration measured at the street level of the street canyon along with a wind rose for the different measurement days and the two-week period of measurements. In the wind rose (Fig. 3b), the wind direction and speed measured at the weather station are shown with an averaging time of 10 min and all the wind directions and speeds present in the two-week data can be seen. In the LDSA concentrations (Fig. 3a), the two-week data showed a strong diurnal pattern as expected at an urban traffic site. Even though the wind

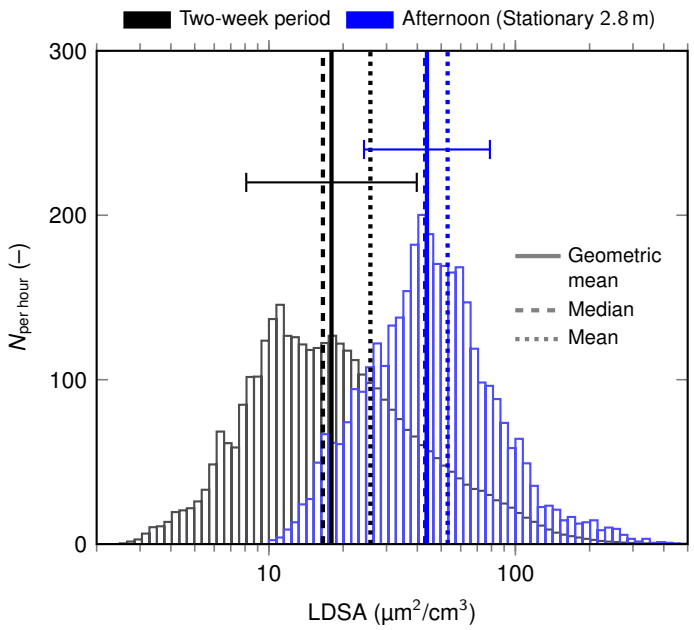

Figure 2: A histogram showing the number of lung deposited surface area (LDSA) concentration values per hour for the two-week period and for the stationary data measured at the height of 2.8 m during an afternoon. Note the logarithmic x-axis. Geometric mean, median, and (arithmetic) mean values are shown for both of the distributions. The horizontal bars represent the geometric standard deviations.

conditions were very different during the two drone measurement days, namely a relatively strong south wind during Day 2 and a much weaker north-east wind during Day 1, the LDSA concentrations measured at the ground level were very similar during these days and close to the two-week averages during daytime. This indicates that the vortex caused by the predominant wind had only a minor influence on the LDSA concentrations compared to the turbulent mixing caused by the traffic. The minor influence of the vortex is not surprising for this sort of a wide avenue street canyon. The wind conditions during the stationary day were close to the wind conditions during Day 1 with respect to street direction and the location of the measurement station. The average LDSA concentrations of the stationary day were also close to the two-week averages and other measurement days during daytime. During night time, there was a much greater deviation in the average LDSA concentrations of different measurement days. The drone measurements and the stationary measurements were carried out during daytime, and the exact measurement periods and the corresponding wind conditions are illustrated with light-colored plots and markers in Fig. 3.

Figure 4 shows the vertical profiles of the LDSA concentration measured with Partector 1 installed into the drone, separately for the two drone measurement days. The deviation of all the measured data points on a logarithmic axis was similar to the examples of the two-week period of measurements and stationary measurements discussed earlier. Thus, the geometric means were used to average the measurements of vertical profiles. As seen in Fig. 4, the shapes of the averaged vertical profiles were similar for both the measurement days. Two different dilution profiles were seen – one of them inside the street canyon with the LDSA

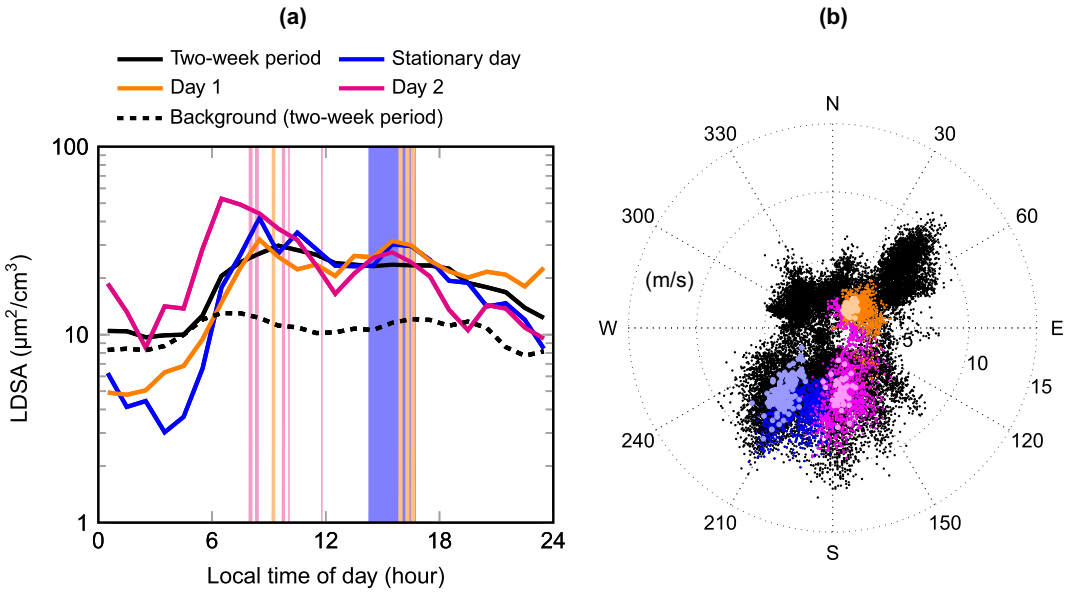

Figure 3: (a) Diurnal variations of the lung deposited surface area (LDSA) concentration measured at the ground level of the street canyon. The data is shown separately for the two-week period, the stationary day, and two drone measurement days. In addition, the diurnal variation measured at the background station corresponding to the two-week period is plotted with a dashed line. The drone and stationary measurement times are illustrated with the shaded color plots on the background. (b) A wind rose shows the wind direction and speed with an averaging time of 10 min. The data is classified according to the measurement day and the light-colored markers represent the actual measurement times.

concentration approaching the background level in the street canyon, and the other above the rooftop level with the LDSA concentration approaching the urban background. The greatest difference between the data of these two days was observed in the magnitude of the deviation for all the data points and in the averaged profiles right below the rooftop level. During the drone measurements of Day 2, the wind speed was much higher (on average 4.8 m/s) compared to Day 1 (2.0 m/s), which may cause more efficient advection of emissions and more random dilution. In addition, the higher wind seemed to contribute to the breakage of the rooftop level concentration as seen in the averaged vertical profiles during Day 2 (Fig. 4b) but not during Day 1 (Fig. 4a). Another factor affecting this issue was probably the wind direction, which caused the measurement site to be on the leeward side during Day 2 and on the windward side during Day 1. However, the effect of the vortex caused by the predominant wind on the vertical profiles and the LDSA concentrations at the ground level seemed to be insignificant.

The results of the drone measurements can also be observed with respect to the supporting data from the ground level measurements and stationary measurements. Therefore, Fig. 4 shows the geometric means and geometric standard deviations for the two-week data measured at the measurement station, for the stationary measurements at two different heights, and for the ground level data that was measured simultaneously with the drone measurements on both sides of the street canyon. It can be seen that the simultaneous ground level

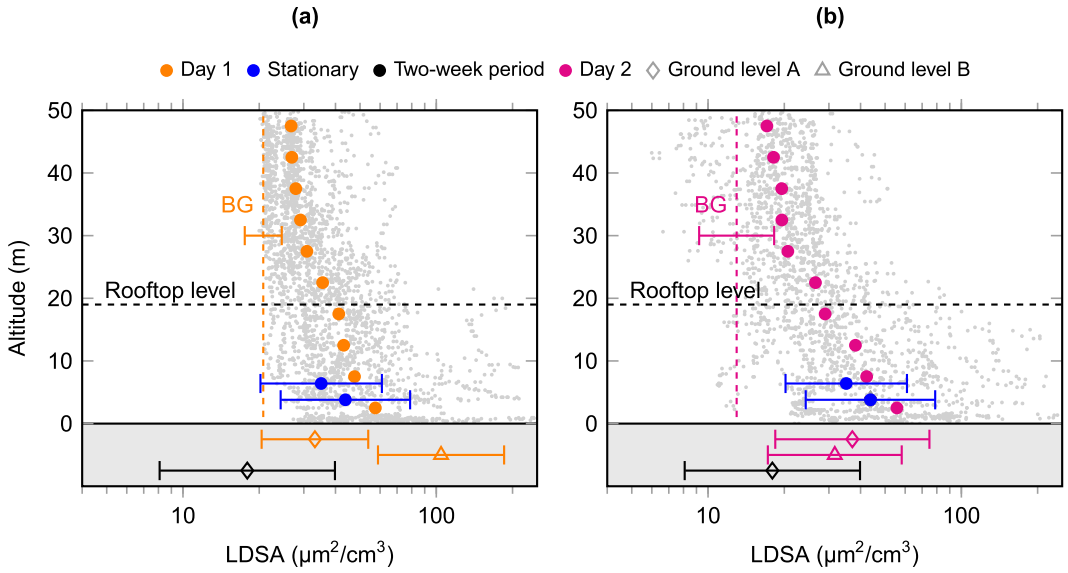

Figure 4: Vertical profiles of lung deposited surface area (LDSA) concentrations for (a) Day 1 and (b) Day 2. All the measured data is presented with gray dots and the geometric means for different altitudes with colored circles. The rooftop level of the closest building is illustrated with a black dashed line. In addition, the geometric means with geometric standard deviations are shown for the two-week data (including also weekends and nights), ground level measurements on both sides of the street canyon simultaneous with the drone measurements, and for the stationary measurements at different heights. The averaged background (BG) concentrations measured at the urban background station simultaneously with the drone measurements are illustrated with colored dashed lines together with the geometric standard deviations.

measurements from the measurement station (A) resulted in smaller LDSA concentrations than the drone measurements carried out right next to the station. The reason for this difference is probably caused by the effect of the measurement station container on the flow field around it. The turbulent mixing caused by traffic may be increased because of the container being located right next to the bus line, which may increase the concentrations behind the corner of the container, while the air at the top of the container is more diluted. Also the air swirl caused by the drone rotors could have an effect on the dispersion of particles around the corner of the measurement station. Interestingly, the different wind conditions during the two measurement days had only a minimal effect on the ground level concentrations measured at this side of the street canyon. This fact supports the insignificance of the vortex and importance of the turbulent mixing caused by traffic on the LDSA concentrations in this sort of a wide avenue canyon. However, on the other side of the street canyon (B), the ground level LDSA concentrations were strongly influenced by the measurement day and the different wind conditions. This asymmetry can most likely be explained by the lack of a container on that side of the street, which allows a more stabilized vortex to affect the concentrations.

The stationary measurements at two different heights supported the vertical LDSA profiles measured with the drone (Fig. 4). The level of the LDSA concentrations was lower in the stationary measurements, as it was in other measurements sampled at the top of

the measurement station container, but the concentration gradient was similar to the drone measurements. Especially, the gradients of the drone measurements on Day 2 and the stationary measurements were close to each other (Fig. 4b). This is reasonable with respect to the wind conditions that were similar during the drone measurements on Day 2 and during the stationary measurements. The comparison between the drone measurements and stationary measurements is important because the air swirl caused by the drone rotors may have an effect on the vertical dispersion of emissions and the concentration gradient. However, the results indicate that this effect was not significant at least during daytime with the presumably high turbulent mixing caused by traffic. In order to analyze this issue from another perspective, we also plotted the vertical profiles measured with the drone separately on ascent and descent (Fig. S3). This analysis showed that, even if the flight direction most probably affected notably the flow field around the drone, it did not have a significant effect on the vertical LDSA profiles. These results are comparable to the measurements and analysis carried out previously by Villa et al. (2017). Of course, the air swirl caused by the drone rotors may occasionally increase or decrease the vertical dispersion of traffic emissions, but with a decent number of repeats the effect seems to be small. This conclusion was also supported by the relatively small and random changes seen in the diurnal variations of drone measurement days when the drone flight times were removed from the ground level measurement data (Fig. S4).

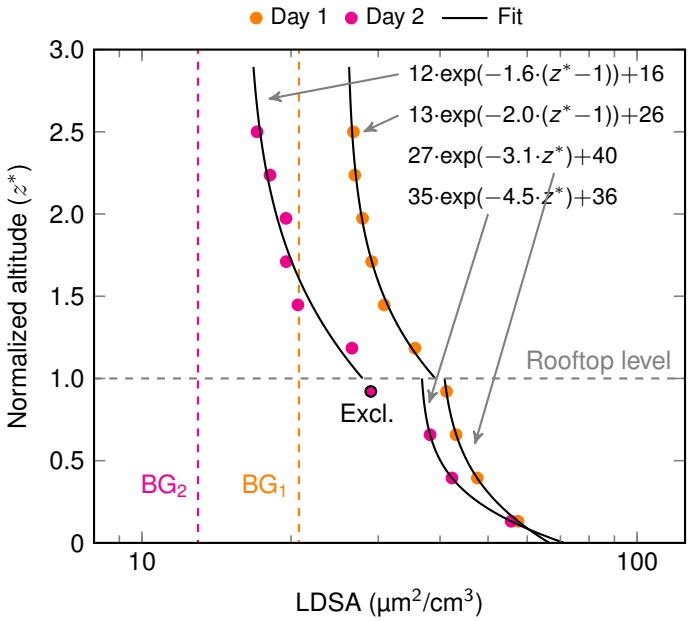

Figure 5: Exponential functions fitted to the measured vertical profiles (geometric mean values) of lung deposited surface area (LDSA) concentrations for two measurement days (colored circles). Separate fits for both the days and two different regions, one in the street canyon and the other over the rooftop level, are shown with functional forms for LDSA concentration in $\mu m^2/cm^3$. The altitude is normalized with the rooftop height ($z^* = z/H$). The rooftop level of the closest building is illustrated with a gray dashed line and the averaged urban background (BG) concentrations measured simultaneously with the drone measurements are illustrated with colored dashed lines.

The exponential functions, described by Eqs. (1) and (2), were used to fit the averaged vertical LDSA concentration profiles. Figure 5 presents the geometric means of the measured LDSA concentrations along with fitted curves for both of the drone measurement days. Additionally, the measured urban background (BG) concentrations are shown. The profiles show that the vertical dispersion and dilution were different inside the canyon compared to the region above the rooftop level. Inside the canyon, profiles were similar for both the days, with the exception of a slight difference in the exponential decay. Analogously, the profiles over the rooftop were similar with each other, especially with respect to the exponential decay and dilution. The largest difference was in the urban background concentrations, which mostly explains the shift in the LDSA axis. Note that, one measurement point for Day 2 inside the canyon closest to the rooftop was excluded from the fit, since, as discussed earlier, the wind speed was higher during Day 2, which probably resulted in the breakage of the rooftop level concentration. This claim and the exclusion of the point is supported by the fact that the excluded point seems to align well with the Day 2 data points above the rooftop level, if the curve is extended to lower altitudes. Moreover, this indicates that a complex mixing phenomenon occurs in the region near the rooftop level, when two different kind of air masses are colliding, and results in effectively lower canyon height during Day 2. By taking into account the effectively lower canyon height, the fit with two parts would also become continuous.

Table 1 displays the values obtained for the fitted parameters along with the 95 % confidence bounds. In comparison of these parameter values, the street canyon background concentrations $C_{\mathrm{BG,str}}$ were close to each other for both of the days, and the ground level concentration resulting from the ground level emissions $C_{\mathrm{E,grd}}$ showed only a small variation (8 $\mu m^2/cm^3$) between the days. Moreover, the largest difference was in the decay coefficients k, which were higher for Day 2. This difference is probably due to the stronger wind during that day. On the other hand, the values for k were still relatively close to each other, and, for this reason, it can be hypothesized that the turbulent mixing caused by traffic was a dominant dispersion mechanism. The rooftop level concentrations $C_{\mathrm{E,rft}}$ and the decay coefficients k were almost identical for the two measurement days, whereas the differences in the urban background $C_{\mathrm{BG,urb}}$ explained the differences in the vertical profiles above the rooftop level. Similar differences were also found in the measured urban background concentrations, which were 20.75 and 12.97 $\mu m^2/cm^3$ for Day 1 and Day 2, respectively. Although the fits on the drone data predicted higher urban background concentrations than the measurement, they agreed well with each other. The goodness of the fits seen in the correlation coefficient values (R^2) supports the chosen functional forms for both the regions above and below the rooftop level.

In Table 1, the exponential decay coefficients obtained in this study are compared to values found in the literature. These literature values have been determined for different gaseous compounds, including nitrogen oxides NO_x (Capannelli et al., 1977), tracer gas ethane C_2H_6 (Hoydysh and Dabberdt, 1988; Dabberdt and Hoydysh, 1991), carbon monoxide CO (Zoumakis, 1995), and benzene (Murena and Vorraro, 2003), as well as, for the mass (Chan and Kwok, 2000) and number (Kumar et al., 2008a; Goel and Kumar, 2016)

Table 1: Comparison of the parameter values of the fitted concentration profiles, see Eqs. (1) and (2), obtained in this study and those reported in the literature. $C_{\mathrm{E,grd}}$ is the concentration at the ground level resulting from the ground level emissions, $C_{\mathrm{E,rft}}$ is the concentration at the rooftop level resulting from street canyon emission, $C_{\mathrm{BG,str}}$ is the street canyon background concentration, $C_{\mathrm{BG,urb}}$ is the urban background concentration, and k as well as k_1 are the decay coefficients. The unit for the concentrations C_i is $\mu\mathrm{m}^2/\mathrm{cm}^3$. The coefficients k marked with an asterisk (*) were calculated using coefficients k_1 and reported canyon heights H ($k = k_1 \cdot H$), and the value marked with a circled asterisk (⊛) was calculated by Murena and Vorraro (2003). The error limits are 95 % confidence bounds, and the R^2 -value is the square of the correlation coefficient. Note the trivial fit ($R^2 = 1$) for Day 2 marked with a dagger (†).

	$C_{\mathrm{E,grd}}$ or $C_{\mathrm{E,rft}}$	$C_{\mathrm{BG,str}}$ or $C_{\mathrm{BG,urb}}$	k	k_1 (m^{-1})	H (m)	R^2
This study, Day 1 *street canyon*	26.83 ± 1.72	39.65 ± 1.46	3.11 ± 0.68	0.1635 ± 0.0353	19	0.9999
This study, Day 2 *street canyon*	34.85	36.39	4.50	0.237	19	1.0000†
This study, Day 1 *above rooftop*	13.22 ± 1.45	25.90 ± 1.19	1.99 ± 0.48	0.1046 ± 0.0251	19	0.9967
This study, Day 2 *above rooftop*	11.73 ± 5.69	16.17 ± 5.27	1.55 ± 1.62	0.0815 ± 0.0850	19	0.9544
Capannelli et al. (1977)			-	0.049 to 0.083	-	-
Hoydysh and Dabberdt (1988)			0.33 to 1.86	-	0.075	0.95 to 1.00
Dabberdt and Hoydysh (1991)			0.3248 to 2.9466	-	0.075	0.949 to 0.997
Zoumakis (1995)			1.18 to 1.86	0.041 to 0.064*	29	0.867 to 0.949
Chan and Kwok (2000)			1.08*	0.036⊛	30	0.9924 to 0.9983
Murena and Vorraro (2003)			2.64 to 5.28*	0.08 to 0.16	33	-
Kumar et al. (2008a)			1.8 to 2.2*	0.10	18 to 22	0.60
Goel and Kumar (2016)			9.24 and 12.72*	0.66 and 2.12	14 and 6	0.86 and 0.99

concentrations of particulate matter. Some of the values have originally been reported as a dimensionless decay coefficient k and others as a decay coefficient k_1 with the unit of m^{-1}. These two values are linked with the canyon height H, and thus, to allow better comparability between the literature values, the coefficients k_1 found in the literature were converted, in this study, to dimensionless k and vice versa by using the canyon heights reported in the original studies. However, Capannelli et al. (1977) did not specify the canyon height, thus conversion to k was not possible. Furthermore, using an extremely small H in wind tunnel experiments yielded unreasonably high k_1 values (Hoydysh and Dabberdt, 1988; Dabberdt and Hoydysh, 1991), and thus, the values are not presented in Table 1.

The values for k in Table 1 varied approximately from 0.3 to 13. In a closer inspection, the values determined for gaseous compounds show only a slight difference when compared to the values for particles. However, it can be said that the k values were slightly higher for particle number concentrations (Kumar et al., 2008a; Goel and Kumar, 2016) and LDSA concentrations (this study). This is reasonable, because particles can coagulate and deposit, which results in a decrease of the concentration, and hence, increase of k. It should still be noted that the studies were performed in various environments, with varying street canyon characteristics. The highest values for k were obtained by Goel and Kumar (2016), who performed the measurements in an open traffic intersection, while the lower values were obtained in closed street canyons. Thus, it seems that the measurement location affects the vertical dispersion more than the particle dynamics. This conclusion is also supported by Pirjola et al. (2012), who concluded that aerosol dynamics had a minor effect in the dispersion.

Afiq et al. (2012) discussed about the high importance of the canyon aspect ratio (AR)

determining the flow field in street canyons and concluded that the air quality is worst during low wind speed situations in deep canyons because of limited air exchange. Furthermore, Murena and Vorraro (2003) suggested that the aspect ratio has also an important role in explaining the concentration profiles in street canyons. They measured concentration profiles in a very deep street canyon (AR = 5.7), while Chan and Kwok (2000) as well as Kumar et al. (2008a) measured in regular canyons with an AR of 1.65 and 1, respectively. In these three studies, the values of k_1 were towards the lower end of the range shown in Table 1. The street canyon of this study was a wider avenue with an AR of 0.45. The values of k_1 were slightly higher for this canyon, which indicates that the open area of the avenue provided better mixing compared to street canyons with higher aspect ratios. Similarly, Goel and Kumar (2016) performed a study in relatively open areas of traffic intersections and found the highest reported values of k_1. To sum up, this comparison of the decay coefficient values k_1 in Table 1 suggests that the parameter values are lower for regular and deep street canyons than for avenues and traffic intersections with more open areas. However, the pattern is not clear, since also meteorological effects are incorporated in the decay coefficient.

The vertical profiles above the rooftop level have not been reported before for particulate matter, and therefore a direct comparison to literature values is not possible. Interestingly, the values of k and k_1 obtained in this study for the region above the rooftop level were still in the same range with the literature values obtained for street canyons. This finding is particularly intriguing, since, at the same time, the dilution process might be caused by a different physical process above the rooftop level compared to the street canyon.

4. Summary and conclusions

The vertical profiles of alveolar lung deposited surface area (LDSA) concentration were measured for the first time in an urban street canyon by using a drone as a moving measurement platform. In spite of different wind conditions, the averaged vertical profiles of LDSA measured during two different days were found to be close to each other. The averaged LDSA concentrations decreased approximately from 60 $\mu m^2/cm^3$ measured close to the ground level to 36–40 $\mu m^2/cm^3$ measured close to the rooftop level of the street canyon, and further to 16–26 $\mu m^2/cm^3$ measured above the rooftop level. The shapes of the measured vertical profiles were in adequate agreement with the exponential functions used for fitting, both in the street canyon and above the rooftop level. The role of turbulent mixing caused by traffic was emphasized compared to the street canyon vortex as a driving force of the dispersion. However, this phenomenon depends on the specific characteristics of a street canyon environment and should not directly be generalized to different microenvironments such as street canyons with higher aspect ratios.

The purpose of this study was to provide high-resolution vertical measurement data for the use of urban regional air quality models, urban planning, and street canyon model verification. In order to increase the relevance of the results, the parameters obtained from the exponential functions fitted to the measurement data were thoroughly compared to previous studies. The comparison was mainly carried out for the decay coefficients of exponential

functions. It should be noted that some studies have reported the coefficients in a dimensionless form related to the dimensionless canyon height and others a form that is related to the absolute altitude. In this study, the values found in the literature were converted to each other and both of them were compared. However, it is not evident, which one of the decay coefficients should be used as a general parameter in street canyon models, or whether there is such a parameter at all. The comparison of the values obtained in this study and the values found in literature showed that the dimensional decay coefficients were lower for regular and deep street canyons than for environments with more open areas, such as avenues and traffic intersections. However, no significant difference was seen between regular and deep canyons for the values found in literature. There is a need of further studies with respect to street canyon modeling and experiments for model verification in order to really understand the phenomenon of vertical dispersion in various street canyon environments.

The high-resolution measurement data and fits of this study showed that the concentration over the rooftop level decreased exponentially approaching the urban background concentration. In a previous modeling study by Kumar et al. (2009b), a computational fluid dynamics (CFD) model, the operational street pollution model (OSPM), and a box-based model predicted zero concentrations above the rooftop level. Thus, more modeling studies are needed to take into account the dispersion of particles and other pollutants in street canyons, and couple that with the dispersion over the rooftop level. Models should be able to explain the dispersion in different scales starting from the source at the ground level to the level where pollutants are fully mixed to the urban background air. The high-resolution measurement data obtained in this study can be then used in the verification of models. In addition, the methodology based on the use of a drone as a moving measurement platform can be used to characterize the vertical profiles in various urban street canyons as such or support model development for example in different meteorological conditions. In this study, the measurements and data analysis indicated that the effect of the air swirl caused by the drone rotors on the vertical dispersion of particles was small, but this is an issue that may also depend on the type of the street canyon environment and weather conditions, and more comparisons to stationary measurements should be carried out in the future.

Acknowledgements

This work was conducted in the INKA-ILMA/EAKR project funded by Tekes, European Union, Helsinki Region Environmental Authority (HSY), City of Tampere, City of Kuopio, Dekati Ltd., Genano Ltd., Nordic Envicon Ltd., Pegasor Ltd., Sandbox Ltd., Suomen Terveysilma, TreLab Ltd., and Vallox Ltd.

Afiq, W. M. Y., Azwadi, C. S. N., Saqr, K. M., 2012. Effects of buildings aspect ratio, wind speed and wind direction on flow structure and pollutant dispersion in symmetric street canyons: A review. International Journal of Mechanical and Materials Engineering 7 (2), 158–165.

Ai, Z., Mak, C., 2015. From street canyon microclimate to indoor environmental quality in naturally ventilated urban buildings: Issues and possibilities for improvement. Building and Environment 94, 489–503.

Beelen, R., Raaschou-Nielsen, O., Stafoggia, M., Andersen, Z., Weinmayr, G., Hoffmann, B., Wolf, K., Samoli, E., Fischer, P., Nieuwenhuijsen, M., Vineis, P., Xun, W., Katsouyanni, K., Dimakopoulou, K., Oudin, A., Forsberg, B., Modig, L., Havulinna, A., Lanki, T., Turunen, A., Oftedal, B., Nystad, W., Nafstad, P., De Faire, U., Pedersen, N., Östenson, C.-G., Fratiglioni, L., Penell, J., Korek, M., Pershagen, G., Eriksen, K., Overvad, K., Ellermann, T., Eeftens, M., Peeters, P., Meliefste, K., Wang, M., Bueno-De-Mesquita, B., Sugiri, D., Krämer, U., Heinrich, J., De Hoogh, K., Key, T., Peters, A., Hampel, R., Concin, H., Nagel, G., Ineichen, A., Schaffner, E., Probst-Hensch, N., Künzli, N., Schindler, C., Schikowski, T., Adam, M., Phuleria, H., Vilier, A., Clavel-Chapelon, F., Declercq, C., Grioni, S., Krogh, V., Tsai, M.-Y., Ricceri, F., Sacerdote, C., Galassi, C., Migliore, E., Ranzi, A., Cesaroni, G., Badaloni, C., Forastiere, F., Tamayo, I., Amiano, P., Dorronsoro, M., Katsoulis, M., Trichopoulou, A., Brunekreef, B., Hoek, G., 2014. Effects of long-term exposure to air pollution on natural-cause mortality: An analysis of 22 European cohorts within the multicentre ESCAPE project. The Lancet 383 (9919), 785–795.

Berkowicz, R., 2000. OSPM - A Parameterised Street Pollution Model. Environmental Monitoring and Assessment 65 (1-2), 323–331.

Brady, J. M., Stokes, M. D., Bonnardel, J., Bertram, T. H., 2016. Characterization of a quadrotor unmanned aircraft system for aerosol-particle-concentration measurements. Environmental Science & Technology 50 (3), 1376–1383.

Brown, D., Wilson, M., MacNee, W., Stone, V., Donaldson, K., 2001. Size-dependent proinflammatory effects of ultrafine polystyrene particles: A role for surface area and oxidative stress in the enhanced activity of ultrafines. Toxicology and Applied Pharmacology 175 (3), 191–199.

Capannelli, G., Gollo, E., Munari, S., Ratto, G., 1977. Nitrogen oxides: Analysis of urban pollution in the city of genoa. Atmospheric Environment (8), 719–727.

Chan, L. Y., Kwok, W. S., 2000. Vertical dispersion of suspended particulates in urban area of hong kong. Atmospheric Environment 34 (26), 4403–4412.

Cheng, Z., Luo, L., Wang, S., Wang, Y., Sharma, S., Shimadera, H., Wang, X., Bressi, M., de Miranda, R., Jiang, J., Zhou, W., Fajardo, O., Yan, N., Hao, J., 2016. Status and characteristics of ambient PM2.5 pollution in global megacities. Environment International 89-90, 212–221.

Dabberdt, W. F., Hoydysh, W. G., 1991. Street canyon dispersion: Sensitivity to block shape and entrainment. Atmospheric Environment 25 (7), 1143–1153.

Elston, J., Argrow, B., Stachura, M., Weibel, D., Lawrence, D., Pope, D., 2015. Overview of small fixed-wing unmanned aircraft for meteorological sampling. Journal of Atmospheric and Oceanic Technology 32 (1), 97–115.

Fierz, M., Houle, C., Steigmeier, P., Burtscher, H., 2011. Design, calibration, and field performance of a miniature diffusion size classifier. Aerosol Science and Technology 45 (1), 1–10.

Fierz, M., Meier, D., Steigmeier, P., Burtscher, H., 2014. Aerosol measurement by induced currents. Aerosol Science and Technology 48 (4), 350–357.

Goel, A., Kumar, P., 2016. Vertical and horizontal variability in airborne nanoparticles and their exposure around signalised traffic intersections. Environmental Pollution 214, 54–69.

Hoydysh, W. G., Dabberdt, W. F., 1988. Kinematics and dispersion characteristics of flows in asymmetric street canyons. Atmospheric Environment 22 (12), 2677–2689.

Huang, C., 1979. A theory of dispersion in turbulent shear flow. Atmospheric Environment (1967) 13 (4), 453 – 463.

Imhof, D., Weingartner, E., Vogt, U., Dreiseidler, A., Rosenbohm, E., Scheer, V., Vogt, R., Nielsen, O., Kurtenbach, R., Corsmeier, U., Kohler, M., Baltensperger, U., 2005. Vertical distribution of aerosol particles and NOx close to a motorway. Atmospheric Environment 39 (31), 5710–5721.

Järvi, L., Hannuniemi, H., Hussein, T., Junninen, H., Aalto, P., Hillamo, R., Mäkelä, T., Keronen, P., Siivola, E., Vesala, T., Kulmala, M., 2009. The urban measurement station SMEAR II: Continuous monitoring of air pollution and surface-atmosphere interactions in Helsinki, Finland. Boreal Environment Research 14, 86–109.

Järvinen, A., Aitomaa, M., Rostedt, A., Keskinen, J., Yli-Ojanperä, J., 2014. Calibration of the new electrical low pressure impactor (ELPI+). Journal of Aerosol Science 69, 150–159.

Järvinen, A., Kuuluvainen, H., Niemi, J., Saari, S., Dal Maso, M., Pirjola, L., Hillamo, R., Janka, K., Keskinen, J., Rönkkö, T., 2015. Monitoring urban air quality with a diffusion charger based electrical particle sensor. Urban Climate 14, 441–456.

Kukkonen, J., Valkonen, E., Walden, J., Koskentalo, T., Aarnio, P., Karppinen, A., Berkowicz, R., Kartastenpää, R., 2001. A measurement campaign in a street canyon in Helsinki and comparison of results with predictions of the OSPM model. Atmospheric Environment 35 (2), 231–243.

Kumar, P., Fennell, P., Britter, R., 2008a. Measurements of particles in the 5–1000nm range close to road level in an urban street canyon. Science of the Total Environment 390 (2), 437–447.

565 Kumar, P., Fennell, P., Hayhurst, A., Britter, R., 2009a. Street versus rooftop level con-
566 centrations of fine particles in a Cambridge street canyon. Boundary-Layer Meteorology
567 131 (1), 3–18.

568 Kumar, P., Fennell, P., Langley, D., Britter, R., 2008b. Pseudo-simultaneous measurements
569 for the vertical variation of coarse, fine and ultrafine particles in an urban street canyon.
570 Atmospheric Environment 42 (18), 4304–4319.

571 Kumar, P., Garmory, A., Ketzel, M., Berkowicz, R., Britter, R., 2009b. Comparative study of
572 measured and modelled number concentrations ofnanoparticles in an urban street canyon.
573 Atmospheric Environment 43 (4), 949–958.

574 Kumar, P., Ketzel, M., Vardoulakis, S., Pirjola, L., Britter, R., 2011. Dynamics and disper-
575 sion modelling of nanoparticles from road traffic in the urban atmospheric environment–A
576 review. Journal of Aerosol Science 42 (9), 580–603.

577 Kuuluvainen, H., Rönkkö, T., Järvinen, A., Saari, S., Karjalainen, P., Lähde, T., Pirjola, L.,
578 Niemi, J., Hillamo, R., Keskinen, J., 2016. Lung deposited surface area size distributions
579 of particulate matter in different urban areas. Atmospheric Environment 136, 105–113.

580 Lelieveld, J., Evans, J., Fnais, M., Giannadaki, D., Pozzer, A., 2015. The contribution of
581 outdoor air pollution sources to premature mortality on a global scale. Nature 525 (7569),
582 367–371.

583 Marini, S., Buonanno, G., Stabile, L., Avino, P., 2015. A benchmark for numerical scheme
584 validation of airborne particle exposure in street canyons. Environmental Science and
585 Pollution Research 22 (3), 2051–2063.

586 Monks, P., Granier, C., Fuzzi, S., Stohl, A., Williams, M., Akimoto, H., Amann, M., Bak-
587 lanov, A., Baltensperger, U., Bey, I., Blake, N., Blake, R., Carslaw, K., Cooper, O.,
588 Dentener, F., Fowler, D., Fragkou, E., Frost, G., Generoso, S., Ginoux, P., Grewe, V.,
589 Guenther, A., Hansson, H., Henne, S., Hjorth, J., Hofzumahaus, A., Huntrieser, H.,
590 Isaksen, I., Jenkin, M., Kaiser, J., Kanakidou, M., Klimont, Z., Kulmala, M., Laj, P.,
591 Lawrence, M., Lee, J., Liousse, C., Maione, M., McFiggans, G., Metzger, A., Mieville, A.,
592 Moussiopoulos, N., Orlando, J., O'Dowd, C., Palmer, P., Parrish, D., Petzold, A., Platt,
593 U., Pöschl, U., Prevot, A., Reeves, C., Reimann, S., Rudich, Y., Sellegri, K., Steinbrecher,
594 R., Simpson, D., ten Brink, H., Theloke, J., van der Werf, G., Vautard, R., Vestreng, V.,
595 Vlachokostas, C., von Glasow, R., 2009. Atmospheric composition change – global and
596 regional air quality. Atmospheric Environment 43 (33), 5268–5350.

597 Murena, F., Vorraro, F., 2003. Vertical gradients of benzene concentration in a deep street
598 canyon in the urban area of Naples. Atmospheric Environment 37 (35), 4853–4859.

599 Oberdörster, G., Oberdörster, E., Oberdörster, J., 2005. Nanotoxicology: An emerging dis-
600 cipline evolving from studies of ultrafine particles. Environmental Health Perspectives
601 113 (7), 823–839.

Pakkanen, T. A., Kerminen, V.-M., Loukkola, K., Hillamo, R. E., Aarnio, P., Koskentalo, T., Maenhaut, W., 2003. Size distributions of mass and chemical components in street-level and rooftop PM1 particles in Helsinki. Atmospheric Environment 37 (12), 1673–1690.

Pant, P., Harrison, R., 2013. Estimation of the contribution of road traffic emissions to particulate matter concentrations from field measurements: A review. Atmospheric Environment 77, 78–97.

Pirjola, L., Lähde, T., Niemi, J., Kousa, A., Rönkkö, T., Karjalainen, P., Keskinen, J., Frey, A., Hillamo, R., 2012. Spatial and temporal characterization of traffic emissions in urban microenvironments with a mobile laboratory. Atmospheric Environment 63, 156–167.

Pirjola, L., Niemi, J., Saarikoski, S., Aurela, M., Enroth, J., Carbone, S., Saarnio, K., Kuuluvainen, H., Kousa, A., Rönkkö, T., Hillamo, R., 2017. Physical and chemical characterization of urban winter-time aerosols by mobile measurements in Helsinki, Finland. Atmospheric Environment 158, 60–75.

Putaud, J.-P., Raes, F., Van Dingenen, R., Brüggemann, E., Facchini, M.-C., Decesari, S., Fuzzi, S., Gehrig, R., Hülin, C., Laj, P., Lorbeer, G., Maenhaut, W., Mihalopoulos, N., Müller, K., Querol, X., Rodriguez, S., Schneider, J., Spindler, G., Ten Brink, H., Torseth, K., Wiedensohler, A., 2004. A european aerosol phenomenology - 2: Chemical characteristics of particulate matter at kerbside, urban, rural and background sites in europe. Atmospheric Environment 38 (16), 2579–2595.

Qin, Y., Kot, S., 1993. Dispersion of vehicular emission in street canyons, Guangzhou City, South China (P.R.C.). Atmospheric Environment. Part B, Urban Atmosphere 27 (3), 283–291.

Reche, C., Viana, M., Brines, M., Perez, N., Beddows, D., Alastuey, A., Querol, X., 2015. Determinants of aerosol lung-deposited surface area variation in an urban environment. Science of the Total Environment 517, 38–47.

Rotstayn, L., Keywood, M., Forgan, B., Gabric, A., Galbally, I., Gras, J., Luhar, A., McTainsh, G., Mitchell, R., Young, S., 2009. Possible impacts of anthropogenic and natural aerosols on Australian climate: A review. International Journal of Climatology 29 (4), 461–479.

Shi, J., Khan, A., Harrison, R., 1999. Measurements of ultrafine particle concentration and size distribution in the urban atmosphere. Science of the Total Environment 235 (1–3), 51–64.

Silva, R., West, J., Zhang, Y., Anenberg, S., Lamarque, J.-F., Shindell, D., Collins, W., Dalsoren, S., Faluvegi, G., Folberth, G., Horowitz, L., Nagashima, T., Naik, V., Rumbold, S., Skeie, R., Sudo, K., Takemura, T., Bergmann, D., Cameron-Smith, P., Cionni, I., Doherty, R., Eyring, V., Josse, B., Mackenzie, I., Plummer, D., Righi, M., Stevenson, D., Strode, S., Szopa, S., Zeng, G., 2013. Global premature mortality due to anthropogenic

outdoor air pollution and the contribution of past climate change. Environmental Research Letters 8 (3), 1–11.

Väkevä, M., Hämeri, K., Kulmala, M., Lahdes, R., Ruuskanen, J., Laitinen, T., 1999. Street level versus rooftop concentrations of submicron aerosol particles and gaseous pollutants in an urban street canyon. Atmospheric Environment 33 (9), 1385–1397.

Vardoulakis, S., Fisher, B., Pericleous, K., Gonzalez-Flesca, N., 2003. Modelling air quality in street canyons: A review. Atmospheric Environment 37 (2), 155–182.

Vardoulakis, S., Gonzalez-Flesca, N., Fisher, B., 2002. Assessment of traffic-related air pollution in two street canyons in paris: implications for exposure studies. Atmospheric Environment 36 (6), 1025 – 1039.

Villa, T., Jayaratne, E., Gonzalez, L., Morawska, L., 2017. Determination of the vertical profile of particle number concentration adjacent to a motorway using an unmanned aerial vehicle. Environmental Pollution 230, 134–142.

Villa, T. F., Gonzalez, F., Miljievic, B., Ristovski, Z. D., Morawska, L., 2016. An overview of small unmanned aerial vehicles for air quality measurements: Present applications and future prospectives. Sensors 16 (7), 1072.

Vogt, R., Christen, A., Rotach, M., Roth, M., Satyanarayana, A., 2006. Temporal dynamics of CO2 fluxes and profiles over a Central European city. Theoretical and Applied Climatology 84 (1-3), 117–126.

Zoumakis, N. M., 1995. A note on average vertical profiles of vehicular pollutant concentrations in urban street canyons. Atmospheric Environment 29 (24), 3719–3725.